Figure S1

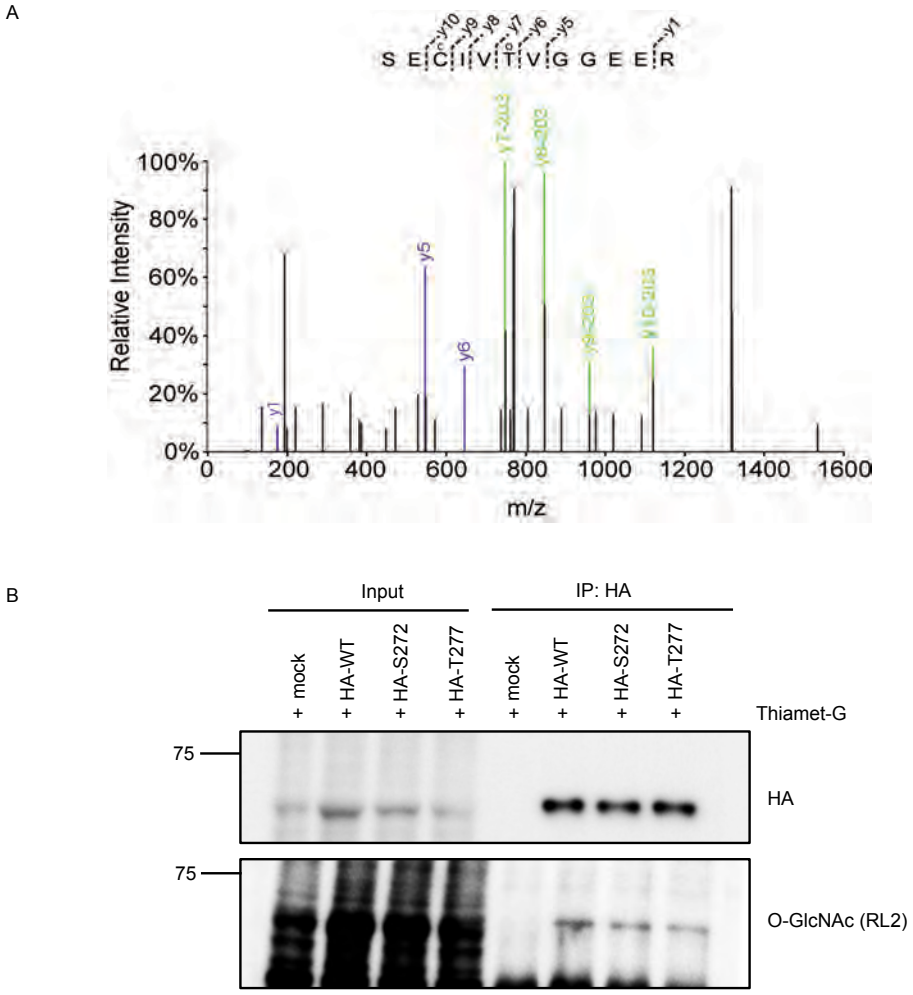

Figure S1. S272 and T277 are candidate sites of gigaxonin O-GlcNAcylation. (A) MS analysis identified two candidate O-GlcNAc sites, S272 and T277, on a monoglycosylated tryptic peptide from gigaxonin. Individual fragment ions annotated with "-203" indicate a gas-phase neutral loss of a single O-GlcNAc moiety. The fragmentation data were insufficient to assign the O-GlcNAc to either S272 or T277 conclusively. Therefore, glycosylation at either site was equally likely in this instance. For illustration purposes, the MS/MS fragmentation spectrum is labeled as if T277 is O-GlcNAcylated. (o: O-GlcNAc, c: carboxyamidomethylcysteine). (B) To validate MS site-mapping data, 293T cells were transfected with WT, S272A or S277A HA-gigaxonin for 46 h, treated with 50 μM Thiamet-G for an additional 26 h, lysed and analyzed by IP-WB. Compared to WT gigaxonin, the S272A and T277A mutants show lower O-GlcNAcylation upon OGA inhibition by Thiamet-G (n=2).

Figure S2

A

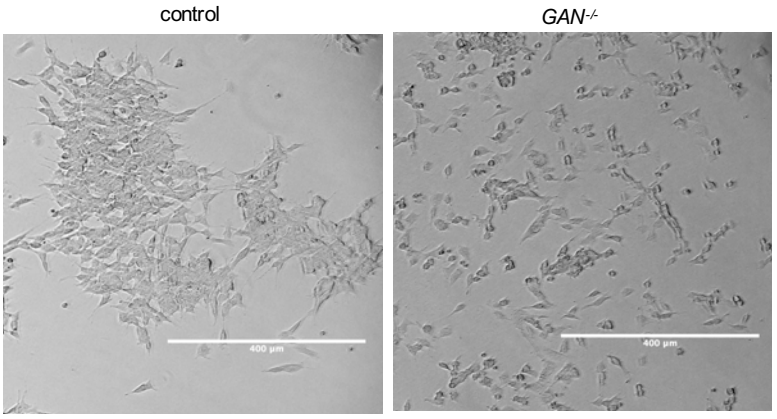

(scale bar: 400 µm)

B

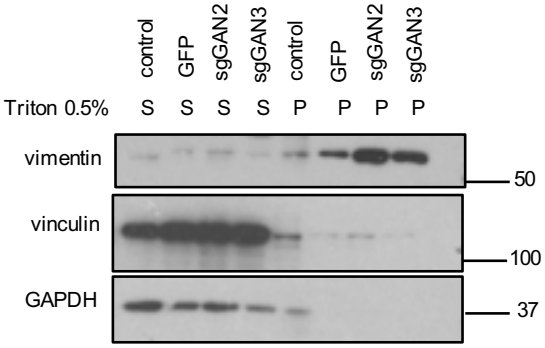

C

BJ5ta

DAPI
vimentin

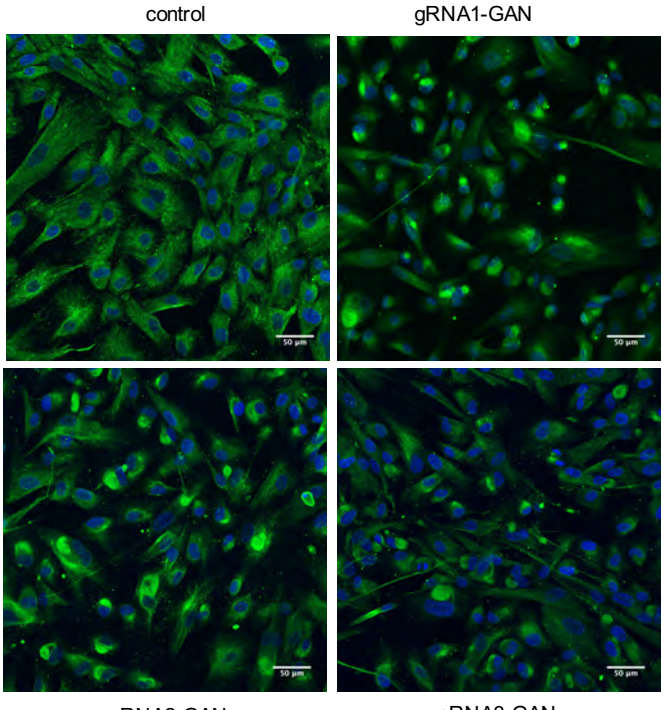

(scale bar: 50 µm)

Figure S2

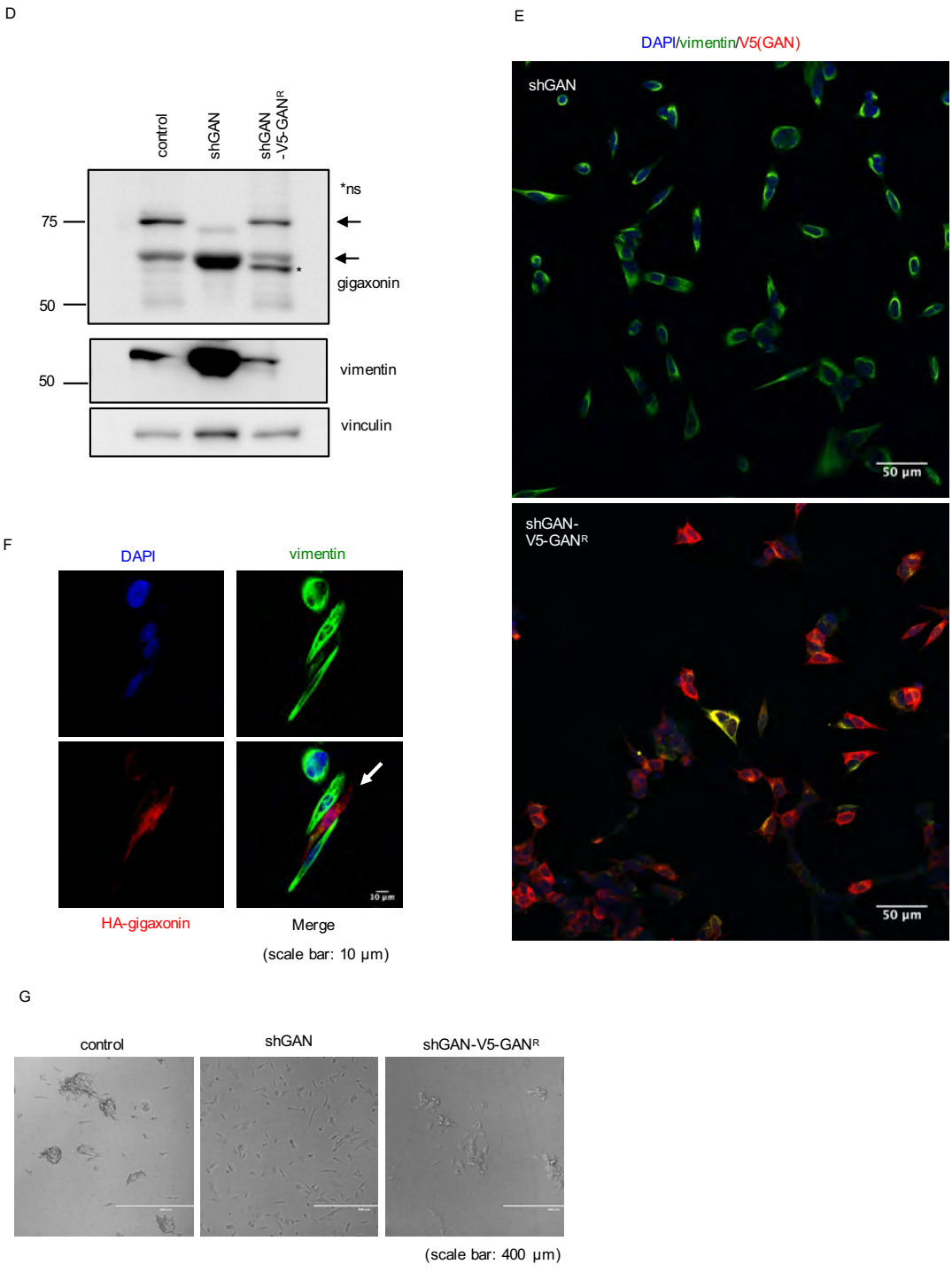

Figure S2. Generation of novel GAN model cell systems by CRISPR-Cas9 genome engineering and shRNA-mediated *GAN* (shGAN) knockdown. (A) Bright field images of control and single cell-derived *GAN*$^{-/-}$ SY-SY5Y clones. Loss of gigaxonin suppresses the clustered growth phenotype observed in control cells. (B) Control SH-SY5Y, GFP-expressing, or two independent *GAN* gRNA-expressing cell lines were lysed in 0.5% Triton buffer. Soluble (S) and insoluble pellet (P) fractions were analyzed

by WB, showing vimentin accumulation in the absence of gigaxonin. (C) BJ5ta cells transfected with either control or one of three independent *GAN* gRNAs were analyzed by IFA (green: vimentin; blue: DAPI). Vimentin forms ovoid, perinuclear aggregates in the absence of gigaxonin. (D) Control or stable *GAN* knockdown (shGAN) SH-SY5Y cells rescued with an shRNA-resistant *GAN* construct (shGAN-V5-GAN^{R}) were lysed and analyzed by WB, confirming loss and restored expression of V5-gigaxonin in shGAN and shGAN-V5-GAN^{R} cells, respectively. (E) shGAN and shGAN-V5-GAN^{R} cells were analyzed by IFA. Re-expression of gigaxonin (V5 tag, red) suppresses the aggregation of vimentin (green). (F) shGAN SH-SY5Y cells were transiently transfected with a control or an HA-gigaxonin expression construct for 72 h and analyzed by IFA. Transient HA-gigaxonin expression (HA, red) clears vimentin aggregates (green). (G) Bright field images of control, shGAN and shGAN-V5-GAN^{R} SH-SY5Y cells. Loss of gigaxonin suppresses the clustered growth phenotype observed in control cells.

Figure S3

A

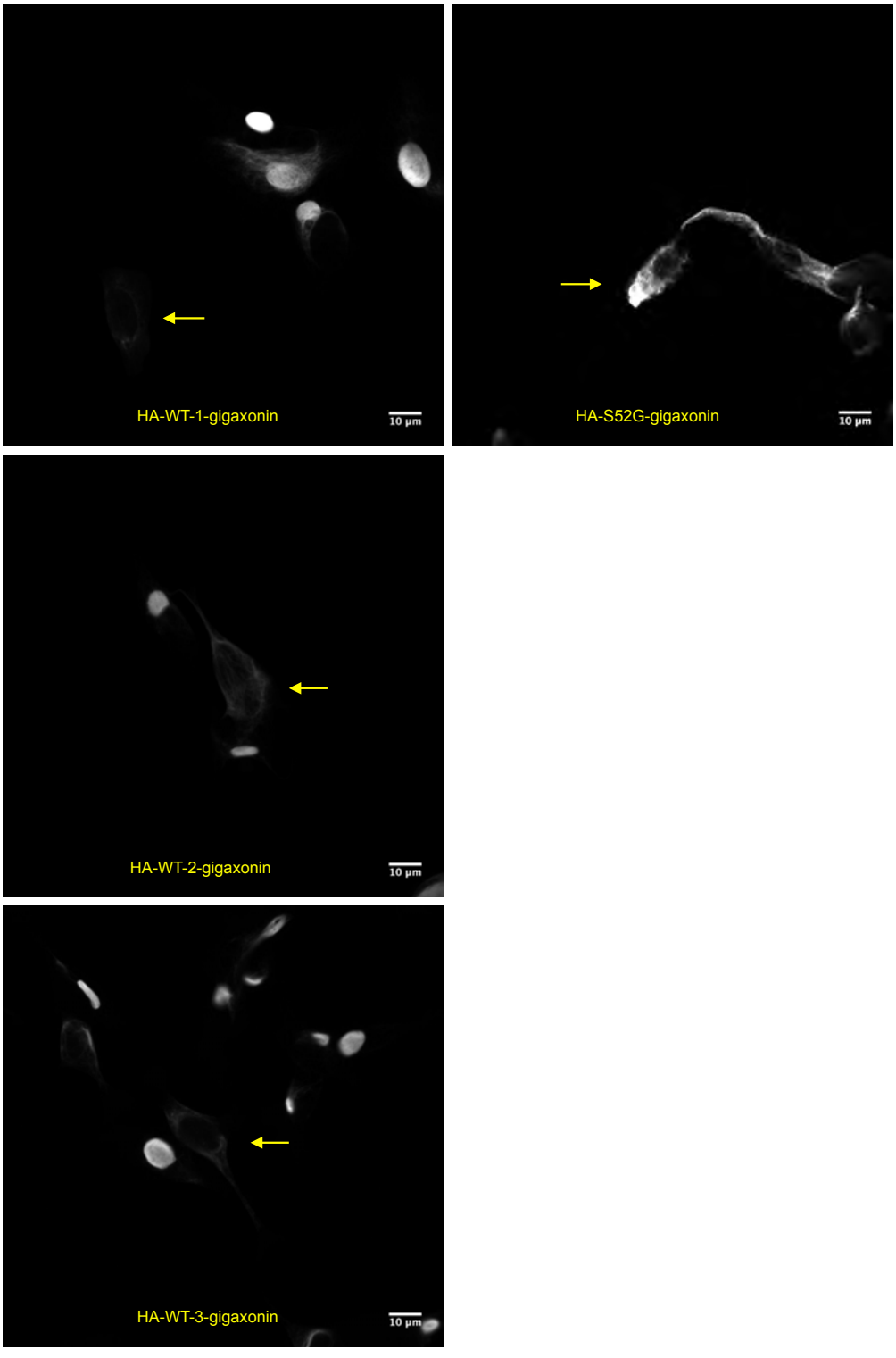
HA-WT-1-gigaxonin
10 μm
HA-S52G-gigaxonin
10 μm
HA-WT-2-gigaxonin
10 μm
HA-WT-3-gigaxonin
10 μm

Figure S3

B

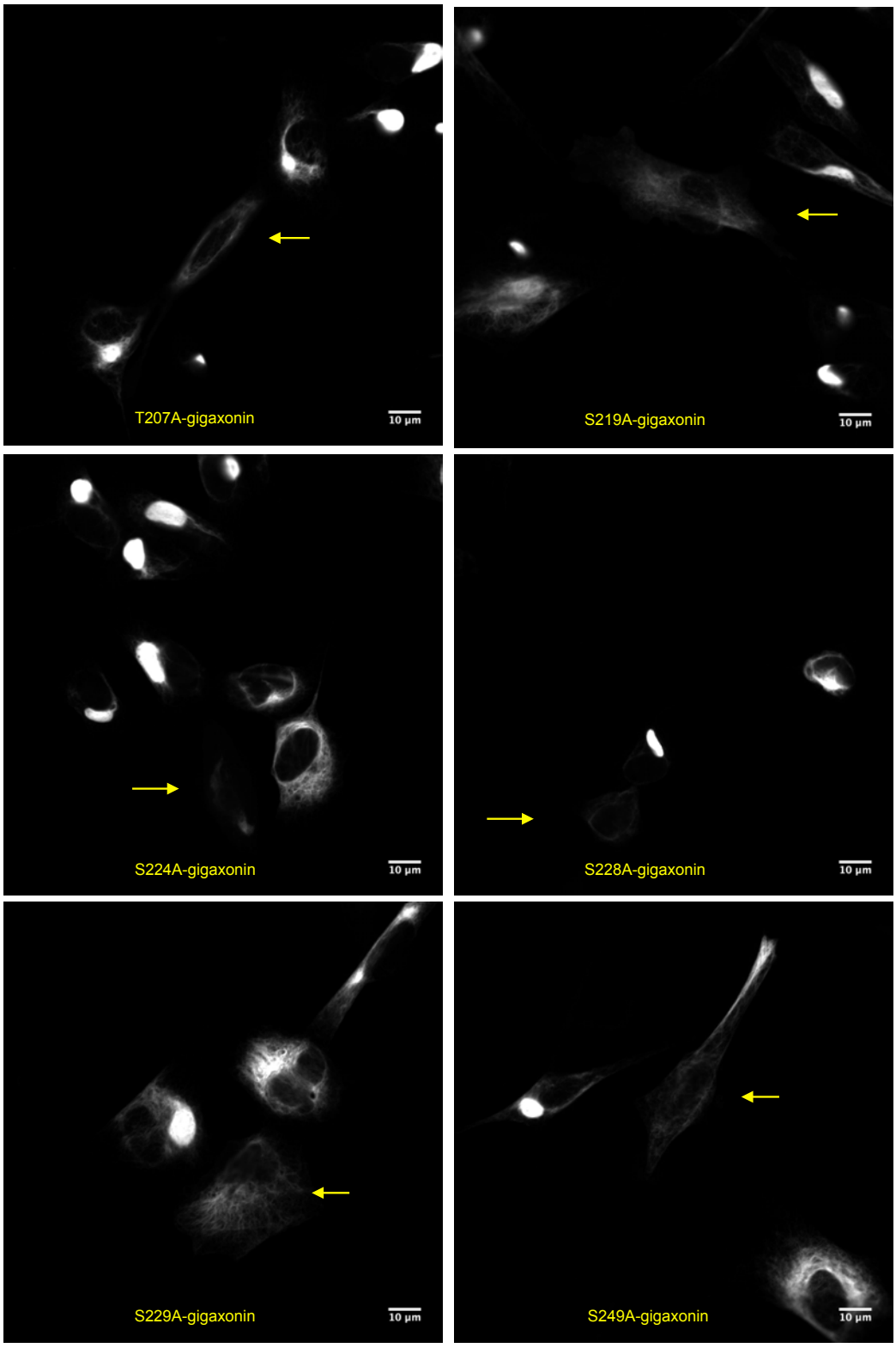
T207A-gigaxonin
10 µm
S219A-gigaxonin
10 µm
S224A-gigaxonin
10 µm
S228A-gigaxonin
10 µm
S229A-gigaxonin
10 µm
S249A-gigaxonin
10 µm

Figure S3

B (continued)

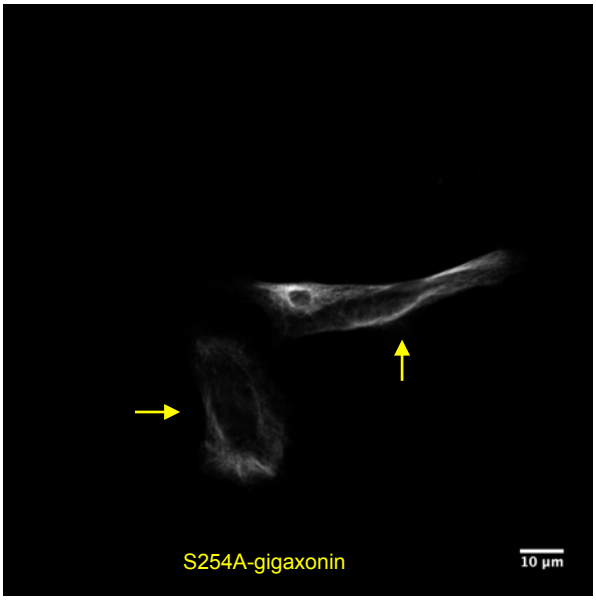

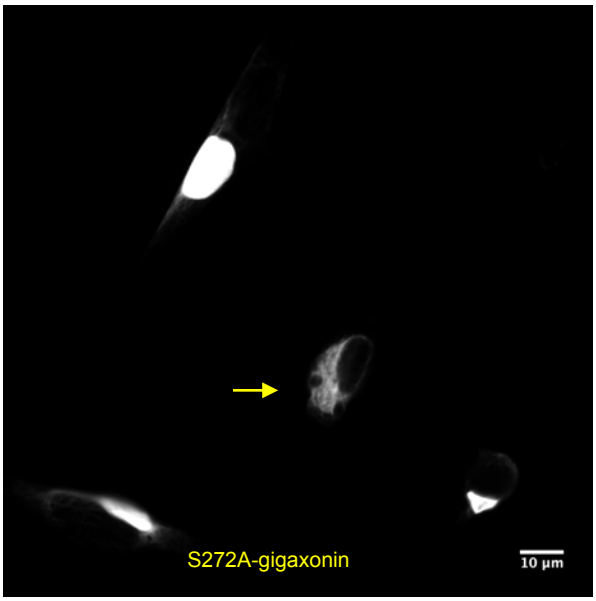

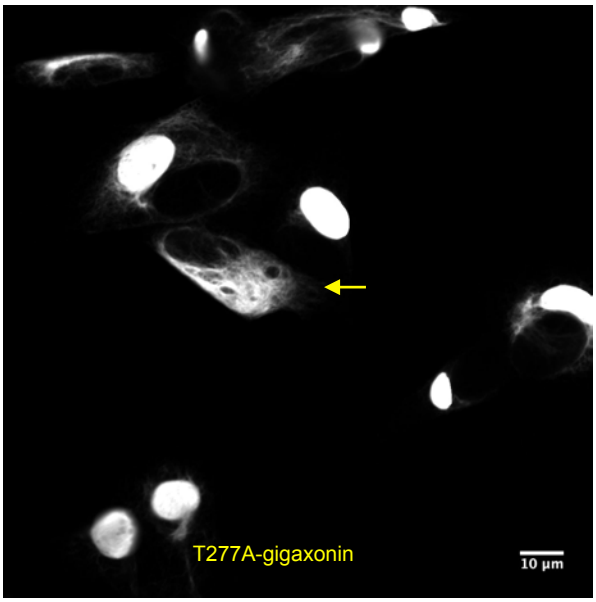

Figure S3

C

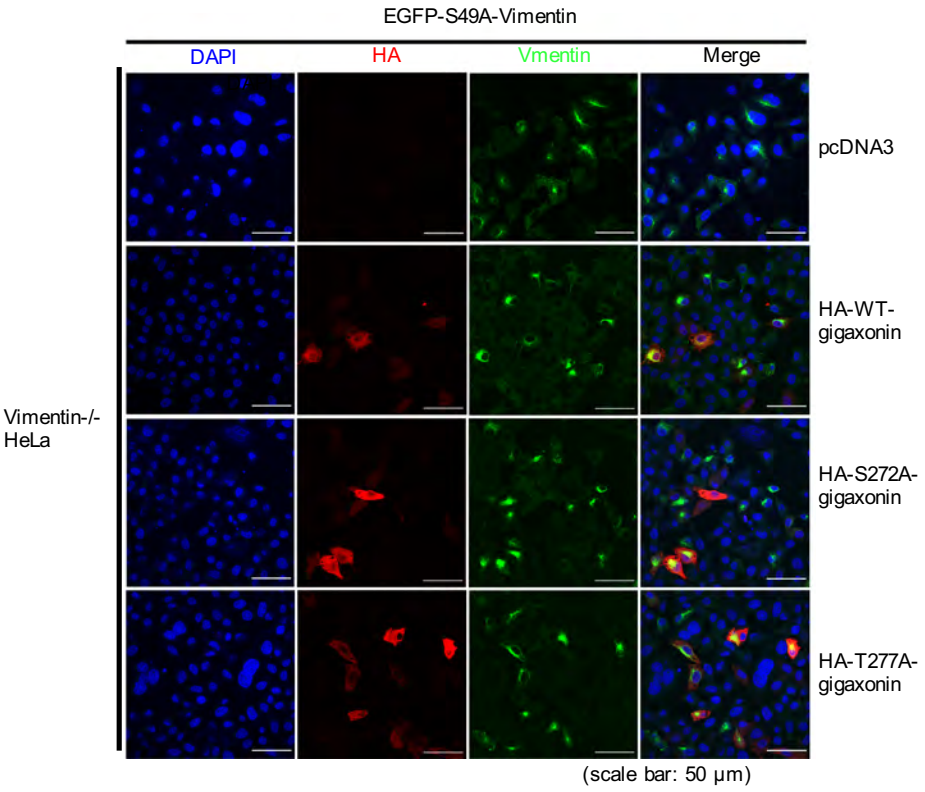

D

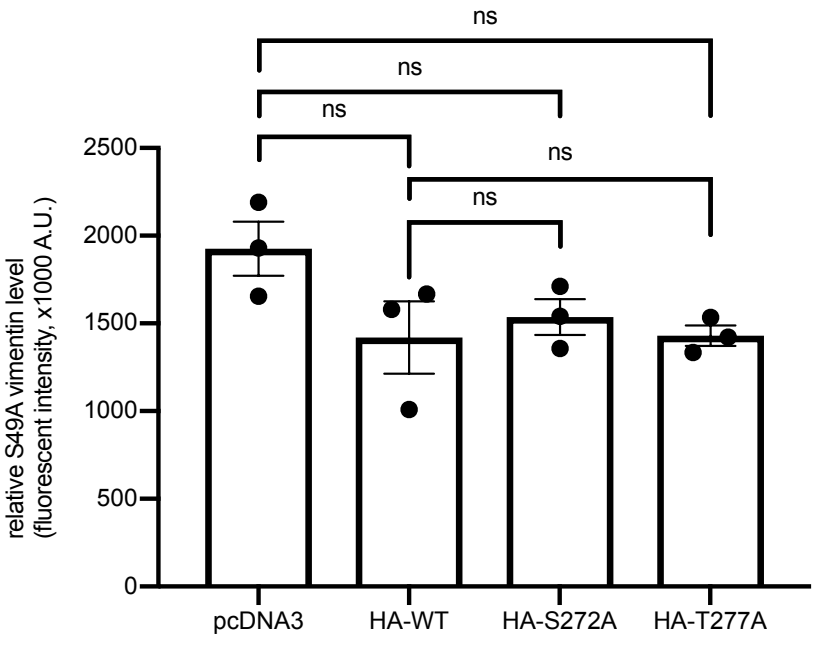

Figure S3. Expression of vimentin in gigaxonin variant-transfected cells. (A-B) Expression of endogenous vimentin in *GAN*$^{-/-}$ SH-SY5Y cells transfected with the indicated *GAN* point-mutants. Yellow arrows indicate transfected cells. (C) Expression of glycosylation site mutant S49A vimentin-EGFP was assessed in

Vimentin$^{-/-}$ HeLa cells transfected with empty vector (pcDNA3) or WT, S272A, or T277A gigaxonin mutants. (D) Quantification of relative expression of S49A vimentin-EGFP in cells transfected with WT or indicated gigaxonin mutants in Fig. S3C. Vimentin-EGFP fluorescence intensity from a total of 80-100 cells with HA-positive signal (or EGFP-positive cells in pcDNA3 group) was measured, normalized to the HA-positive cell number, and averaged across various fields on each cover glass. The mean values of the experimental groups from three biological replicates were analyzed first by one-way ANOVA and then using Tukey's HSD post-hoc test. Error bars represent standard error and p-values < 0.05 were considered statistically significant; ns: non-significant.

Figure S4

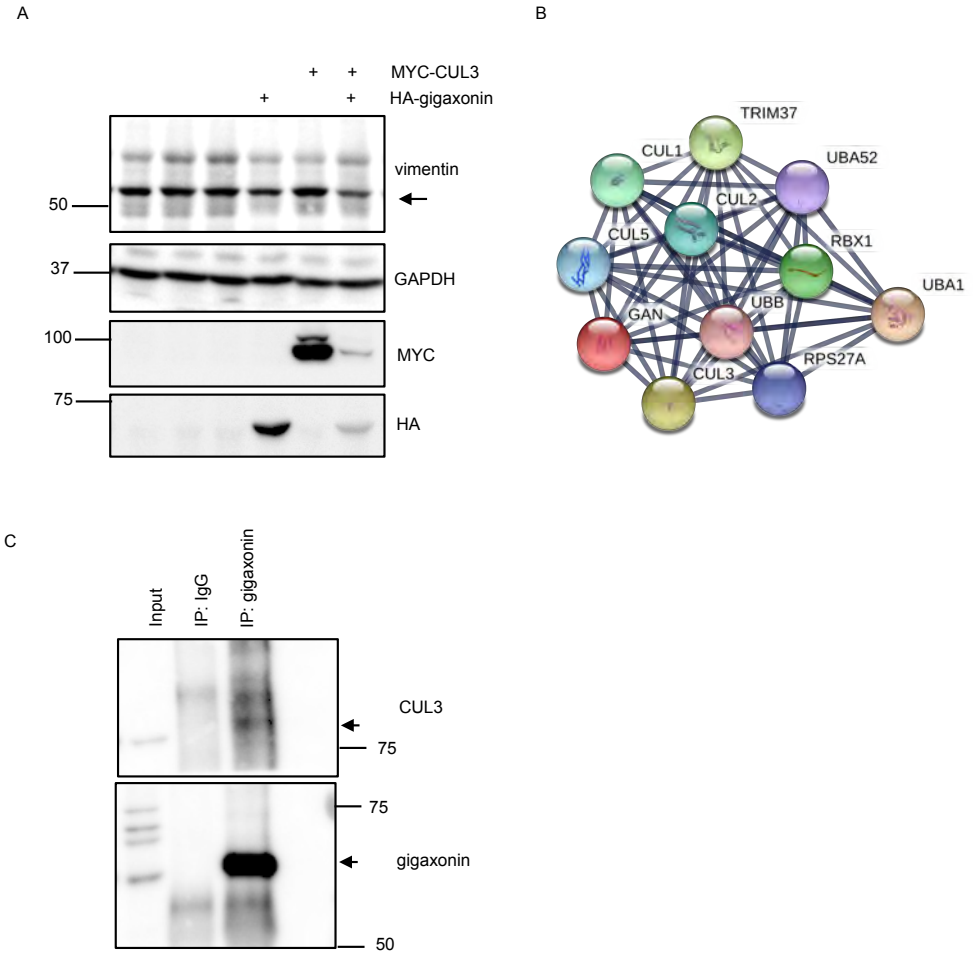

Figure S4. Gigaxonin interacts with CUL3. (A) 293T cells were transfected with expression constructs for HA-gigaxonin, MYC-CUL3 or both, as indicated, for 72 h. Cells were lysed and analyzed by WB. Vimentin is decreased upon the co-expression of HA-gigaxonin and MYC-CUL3. (B) STRING analysis indicates that gigaxonin

interacts with several ubiquitin E3 ligase components. (C) Lysates from MDA-MB-231 cells were subjected to control (IgG) or gigaxonin IP and the indicated proteins were analyzed by WB. Endogenous gigaxonin and CUL3 interact specifically, consistent with previous reports (1).

Figure S5

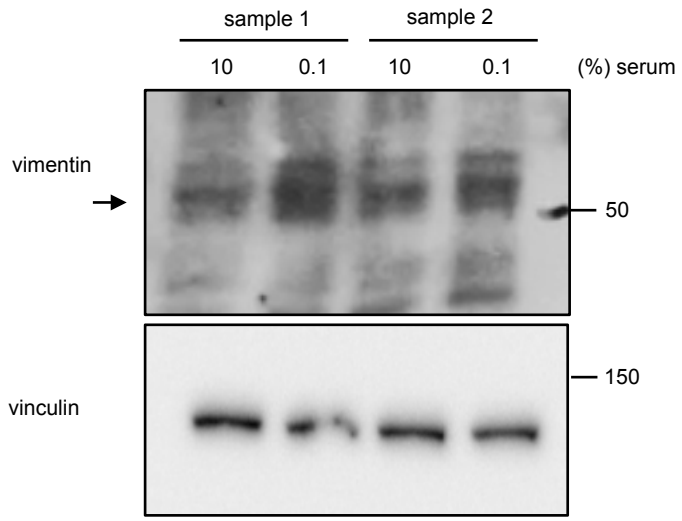

Figure S5. Vimentin protein level is increased upon serum starvation. SH-SY5Y cells were grown under the indicated serum levels (10% or 0.1%) for 72 h, lysed and analyzed by WB. Whole-cell lysates from two biological replicates are shown.

Supplemental reference:

1. Furukawa M, He YJ, Borchers C, and Xiong Y. Targeting of protein ubiquitination by BTB-Cullin 3-Roc1 ubiquitin ligases. *Nat Cell Biol.* 2003;5(11):1001-7.